Frontier of Applied Plasma Technology

Volume 10 No.1 January 2017

Post-He Plasma Treatment on ZnO Thin Film Fabricated by an Atmospheric Pressure Cold Plasma Generator

Xiaoyuan MA*, Takuya TODO*, and Yoshifumi SUZAKI **

*Graduate School, Kagawa University,
**Faculty of Engineering, Kagawa University

pp. 22-26

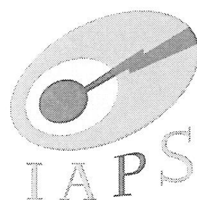

a publication of

Institute of Applied Plasma Science

Post-He Plasma Treatment on ZnO Thin Film Fabricated by Atmospheric Pressure Cold Plasma Generator

Xiaoyuan MA*, Takuya TODO* and Yoshifumi SUZAKI**
*Graduate School, Kagawa University,
**Faculty of Engineering, Kagawa University

Abstract

Zinc oxide (ZnO) films can be used for low-cost transparent electrodes for solar cells and touch panels as alternative materials for Indium Tin Oxide (ITO) films. Recent studies, homogeneous non-equilibrium cold plasma was generated stably using high voltage pulsed power (1 kV, 20 kHz) excitation of He and O_2 gases under atmospheric pressure. By feeding Zn-MOPD (2-methoxy-6-methyl-3,5-heptanedionate-zinc) into this plasma with He carrier gas, transparent flat ZnO films about 190 nm thick were successfully prepared on glass substrates directly under the slit in a cathode at the substrate temperature of 400 ℃. In this paper, we describe the effects of post-He plasma treatment on ZnO thin films. The average transmittance of the films was about 80% with wavelengths ranging from 300 nm to 700 nm. The optical band gap calculated from the absorption edge was 3.40 eV for the as-deposited film. When the treatment time was between 5 min to 60 min, the band gap of the film increased from 3.47 eV to 3.64 eV. X-ray diffraction measurement revealed that as-deposited ZnO films had a c-axis oriented poly-crystalline structure. However, post-He plasma treatment reduced the orientation of the film. By increasing the time of post-He plasma treatment, electrical resistivity decreased from 0.94 Ωcm to 6.2×10^{-2} Ωcm at 60 min. FE-SEM observations show a change in the microstructure of the film. These results suggest that post-He plasma treatment changes the microstructure of the film and then electrical resistivity decreases.

Keywords: Cold plasma, Zinc oxide thin film, Heat treatment, Atmospheric pressure.

1. Introduction

Indium Tin Oxide (ITO) thin films are used for transparent conductive electrodes in display devices and solar cells[1]. Since rare material indium must be imported into Japan, a stable supply is difficult to achieve. ITO thin films are usually prepared by methods such as high temperature chemical vapor deposition (CVD)[2,3], plasma-enhanced chemical vapor deposition (PECVD)[4] and sputtering (SP)[5]. However, expensive vacuum equipment is needed for generating glow discharge plasma. Moreover, the vacuum device causes a restriction in thin film fabrication over large areas. Therefore, alternative materials for ITO thin film have been actively studied. One such alternative material is zinc oxide (ZnO). Because a recycling method of zinc from electric furnace dust has been established, zinc can be stably supplied at a low cost.

In recent studies, homogeneous non-equilibrium cold plasma was generated stably using a radio frequency power or high voltage pulsed power excitation of flowing Ar, He, O_2 and their mixtures at atmospheric pressure[6,7]. In this paper, we describe the effects of post-He plasma treatment on ZnO thin films which have been prepared using atmospheric pressure cold plasma.

2. Experimental Procedure

The fabrication system of our atmospheric pressure cold plasma generator is schematically illustrated in **Fig. 1**. Our plasma generator is composed of an Al cathode with a thin film coating of alumina created by the oxidation process, and a grounded anode of Cu plate. A glass substrate and a heating system were placed on top of the anode plate. A slit (20 mm×1 mm) was made into the cathode (30 mm×50 mm), in order to let He gas flow into the gap between cathode and anode. Also, the anode plate moved with the glass substrate back and forth in the

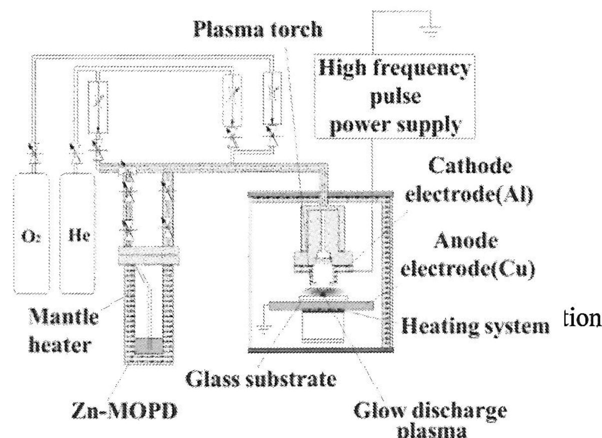

Fig.1 Schematic diagram of the fabrication system.

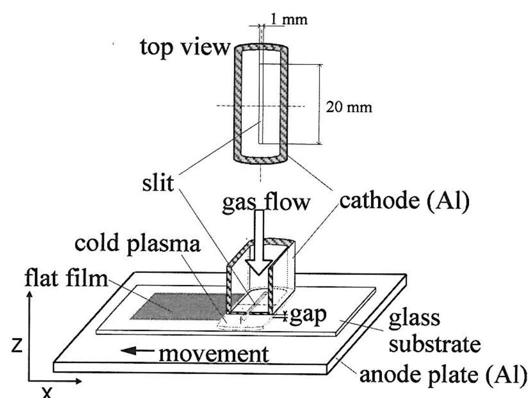

Fig.2 Schematic diagram of movement of the anode plate. The anode moves back and forth during fabrication.

direction perpendicular to the slit in order to prepare flat films with a large area (sweep distance: 10 mm). A schematic diagram of its movement is shown in **Fig. 2**. Atmospheric pressure cold plasma was generated by the flow of He and O_2 gases. The He carrier gas was fed through the inner space of the cathode down to the gap, where it was excited by a high voltage pulse power supply (HVP-20K, Hiden Laboratory Co. Ltd.); then, Zn-MOPD (2-methoxy- 6-methyl- 3,5-heptanedionate- zinc, Ube Industries Ltd.) was vaporized and carried by the He carrier gas flow into the plasma generated in the gap. **Table 1** and **Table 2** list the physical properties of Zn-MOPD and fabrication conditions, respectively. A film about 190 nm thick grew directly under the slit in the cathode with a deposition rate of about 32 nm/min. Post-He

Table 1 Fabrication conditions.

Substrate	Glass
Substrate temperature	400 ℃
Source material	Zn-MOPD (UBE Industries, Ltd.)
Source material temperature	100 ℃
He gas total flow rate	1600 ccm
O_2 gas flow rate	10 ccm
Voltage	1 kV
Sweep speed	1 mm/s
Anode and cathode gap	0.5 mm
Deposition time	60 min

Table 2 Physical properties of Zn-MOPD.

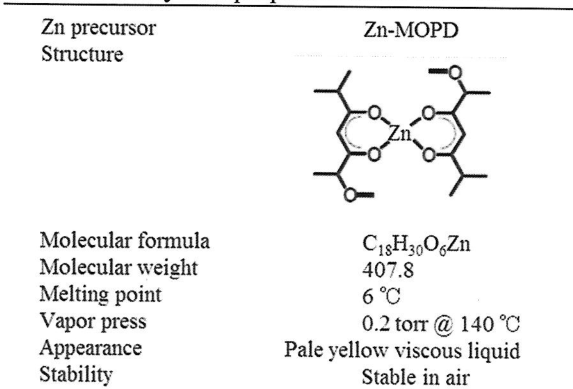

Zn precursor	Zn-MOPD
Structure	
Molecular formula	$C_{18}H_{30}O_6Zn$
Molecular weight	407.8
Melting point	6 ℃
Vapor press	0.2 torr @ 140 ℃
Appearance	Pale yellow viscous liquid
Stability	Stable in air

Table 3 Post-He plasma treatment conditions.

Substrate temperature	400 ℃
He gas flow rate	1600 ccm
Voltage	1 kV
Sweep speed	1 mm/s
Anode and cathode gap	0.5 mm
Treatment time	0 – 60 min

plasma treatment was done for 5 min - 60 min after deposition. **Table 3** lists conditions of the post-He plasma treatment.

Spectral transmittance and reflectance of the film were measured by a spectrophotometer (UV-3150, Shimadzu Corp.). The microstructure of the film was examined by a field emission scanning electron microscope (FE-SEM; S-900s, Hitachi Ltd.) with an accelerating voltage of 15 kV and X-ray diffraction (XRD; XRD6100, Shimadzu Corp.) measurement with Cu-Kα. Resistivity of the films was tested by the four-probe method.

3. Results and Discussion

3.1 Glow discharge region

The range of glow discharge in our experiment is shown in **Figure 3**. The horizontal and vertical axes indicate the O_2 gas flow rate and the voltage of the pulse supply, respectively. Square (▲) and circular (●) data show maximum and minimum values of the glow discharge voltage, respectively. When the O_2 gas flow rate was increased to 10 ccm, stable glow discharge was observed for voltages ranging from 0.4 kV to 4.8 kV. However, above 4.8 kV, unstable streamer discharge was observed instead of glow discharge. Stable discharge can be obtained at a higher voltage with a higher oxygen flow rate. Since oxygen ions in the plasma have high electronegativity they recombine with electrons in the plasma easily. Thus the density of electrons in the plasma is held lower than the limit value for transition to the streamer discharge. Using the cathode with a thin film coating

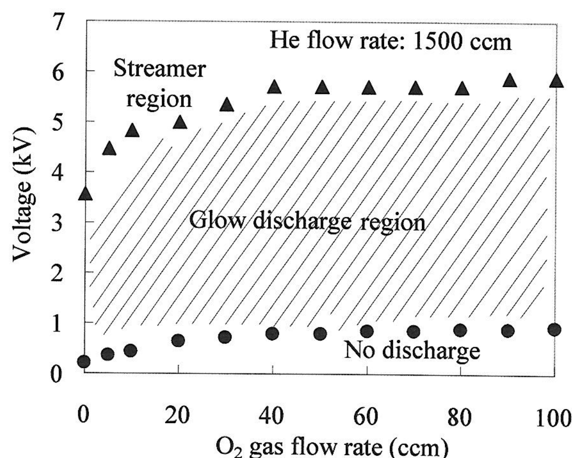

Fig.3 Glow discharge region of the cold plasma generator.

of alumina, it is easier to generate stable glow discharge even if the O_2 gas flow rate is low[8].

Photo of the cathode is shown in **Fig. 4**. The slit (1 mm×20 mm) was prepared on the cathode (30 mm ×50 mm). Typical glow discharge is shown in **Fig. 5**. Bright purple light is shown between the aluminum cathode and the copper anode.

3.2 Transmittance and electrical resistivity

Figure 6 shows the typical spectral transmittance and reflectance of the as-deposited ZnO film and the ZnO films after post-He plasma treatment for 5 min - 60 min. The average transmittance of the films was about 80%; the wavelength ranged from 400 nm to 800 nm. These spectra have absorption edges. When the treatment time increased, the absorption edge shifted to a shorter wavelength. The optical band gap calculated from the absorption edge is 3.40 eV for the as-deposited film. When the post-He plasma treatment time was between 5 min to 60 min, the band gap of the film increased from 3.47 eV to 3.64 eV, which is larger than the value of 3.30 eV (ZnO thin film) reported by C. Lee et al.[9] and Y. Nose et al.[10].

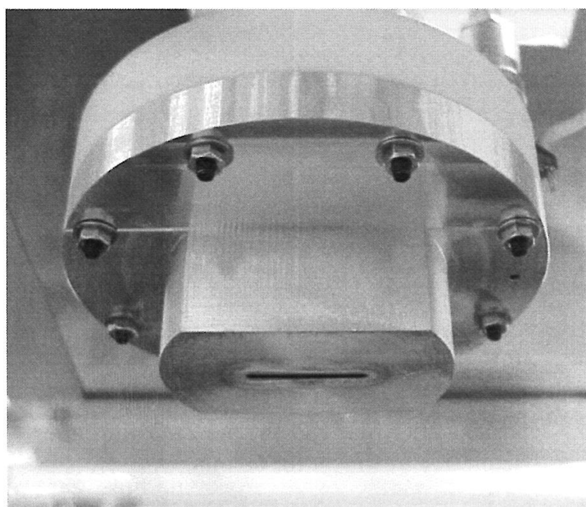

Fig.4 Photo of the cathode (30 mm×50 mm) with the slit (1 mm×20 mm).

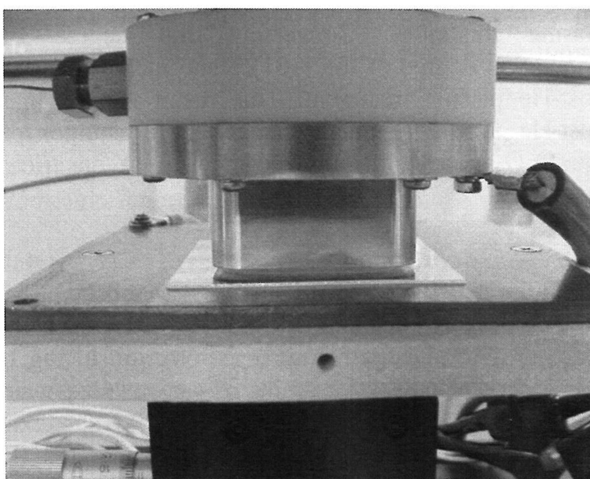

Fig.5 Typical glow discharge. Bright purple light is shown between the aluminum cathode and a glass substrate on the copper anode.

3.3 Electrical Resistivity

Figure 7 shows the electrical resistivity of the ZnO films. The resistivity of the as-deposited films was 0.94 Ωcm. By increasing the post-He plasma treatment time, the resistivity of the films decreased to 6.2×10^{-2} Ωcm with a plasma treatment time of 60 min. In our previous study[11], the resistivity of ZnO films was 1.1×10 Ωcm after annealing at 400℃ for 60 min

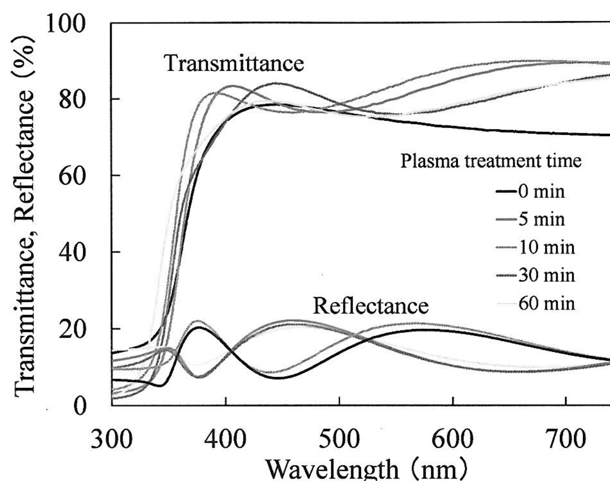

Fig.6 Typical transmittance and reflectance spectra of ZnO films after post-He plasma treatment for 0 min - 60 min. These spectra have absorption edges. When the treatment time increased, the absorption edge shifted to a shorter wavelength. The optical band gap calculated from the absorption edge is 3.40 eV for the as-deposited film. When the post-He plasma treatment time was between 5 min to 60 min, the band gap of the film increased from 3.47 eV to 3.64 eV.

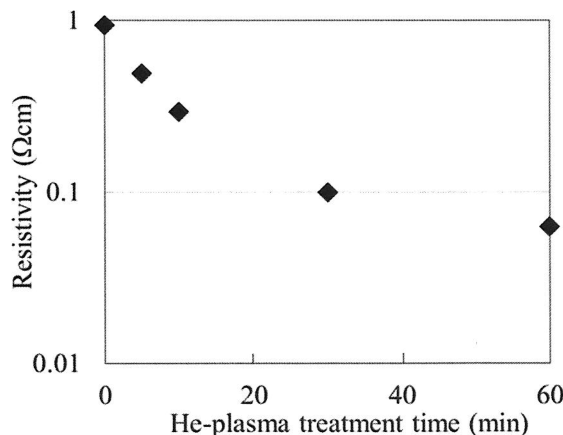

Fig.7 Electrical resistivity of ZnO films after post-He plasma treatment for 0 min - 60 min. By increasing the post-He plasma treatment time, the resistivity of the films decreased to 6.2×10^{-2} Ωcm with a plasma treatment time of 60 min.

without He plasma treatment. This finding suggests that the post-He plasma treatment changes the microstructure of the film and causes electrical resistivity to decrease.

3.4 Analysis of the crystal structure using XRD

Figure 8 shows typical XRD profiles of (a) the as-deposited film and the films treated by the He-plasma for (b) 5 min, (c) 10 min, (d) 30 min and (e) 60 min. The profile in Fig.8 (a) shows peaks for the (100), (002) and (101) planes of hexagonal ZnO crystal. The largest (002) peak shows that the ZnO film has a polycrystalline structure oriented c-axis. Fig.8 (b) - (e) also show peaks for the (100), (002) and (101) planes. The peak for (101) is larger than the other peaks. The largest (101) peak appeared in the profile of the film after post-He plasma treatment for 60 min, as shown in Fig.8 (e). The degree of orientation of the (002) plane and (101) plane of the ZnO thin films for all samples were calculated using the following Lotgering relation[12],

$$F(hkl) = \frac{P(hkl) - P_0(hkl)}{1 - P_0(hkl)} \quad (1)$$

where, $F(hkl)$ is the degree of (hkl) orientation, $P(hkl) = I(hkl)/\Sigma I(hkl)$ and $P_0(hkl) = I_0(hkl)/\Sigma I_0(hkl)$. Here, $I(hkl)$ is the (hkl) peak intensity and $\Sigma I(hkl)$ is the sum of the intensities of all peaks in the ZnO thin films' diffraction spectra data. $I_0(hkl)$ is the (hkl) peak intensity and $\Sigma I_0(hkl)$ is the sum of the intensities of diffraction peaks in the powder diffraction file (JCPDS 36-1451)[13]. The calculated values of

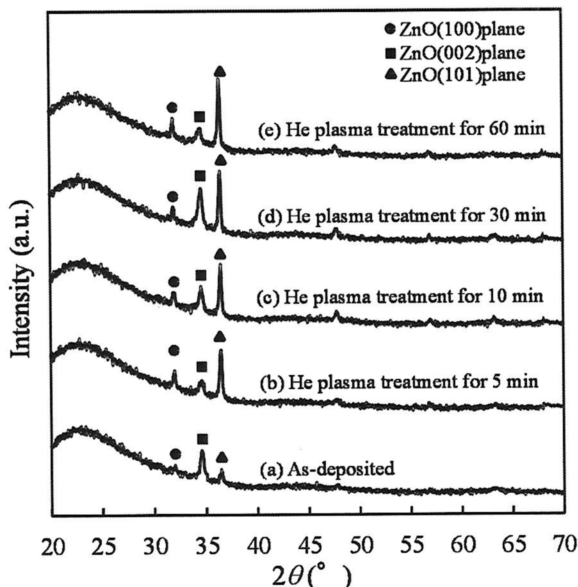

Fig.8 Typical XRD profiles of (a) as-deposited film and the films treated by the He-plasma for (b) 5 min, (c) 10 min, (d) 30 min and (e) 60 min.

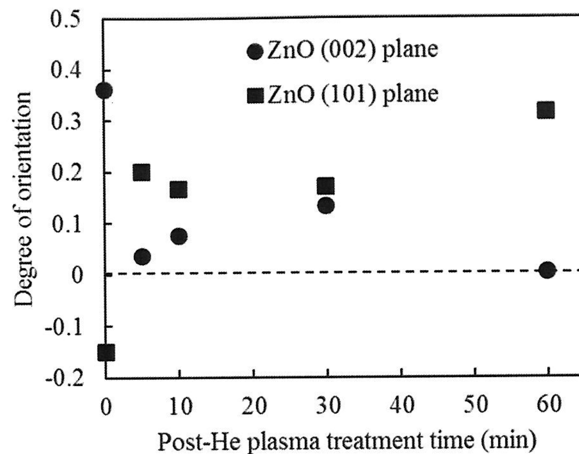

Fig.9 The calculated values of orientation degree of the (002) plane and (101) plane for as-deposited ZnO thin film and ZnO thin films after post-He plasma treatment.

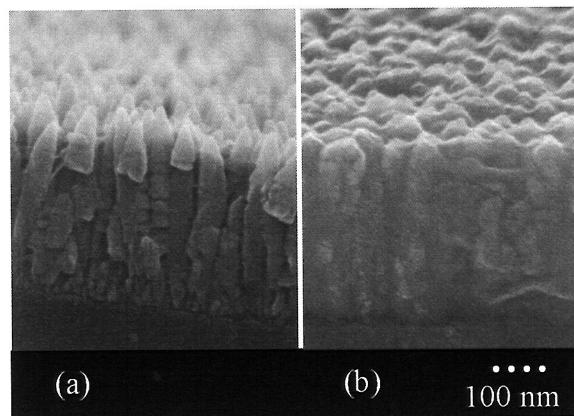

Fig.10 Typical FE-SEM observations of (a) the as-deposited ZnO film and (b) the ZnO film after post-He plasma treatment for 60 min.

orientation degree of the (002) plane and (101) plane for all samples are shown in **Fig. 9**. The degree of orientation of the (002) plane decreased after post-He plasma treatment. Conversely, the degree of orientation degree of the (101) plane increased after post-He plasma treatment. This result reveals that post-He plasma treatment changes the orientation of the ZnO crystal. It might decrease the electrical resistivity.

3.5 FE-SEM observation

Figure 10 shows typical FE-SEM observations of (a) the as-deposited ZnO film and (b) the ZnO film after post-He plasma treatment for 60 min. In Fig.10 (a), conic shaped crystal grains of various sizes were observed on the cross sectional view. Gaps exist between them. However, gaps disappeared and the grain columns were tightly packed with a smooth surface after post-He plasma treatment, as shown in Fig.10 (b). This smooth shape might cause high mobility, which is good for reducing resistivity.

4. Conclusion

Using our atmospheric pressure cold plasma generator, we prepared ZnO films on glass substrates by feeding Zn-MOPD into the plasma, under a substrate temperature of 400 ℃. In this paper, post-He plasma treatment was done and the results are summarized as follows.

(1) A film about 190 nm thick grew directly under the slit in the cathode with a deposition rate of about 32 nm/min.

(2) The average transmittance of the films was about 80%; the wavelength ranged from 400 nm to 800 nm. When treatment time increased, the absorption edge sifted to a shorter wavelength. The optical band gap calculated from the absorption edge was 3.40 eV for the as-deposited film. When the treatment time was between 5 min to 60 min, the band gap of the film increased from 3.47 eV to 3.64 eV.

(3) The resistivity of the as-deposited film is 0.94 Ωcm. By increasing the post-He plasma treatment time, the resistivity of the film decreased to 6.2×10^{-2} Ωcm at a post-He plasma treatment time of 60 min.

(4) As-deposited ZnO film has a polycrystalline structure-oriented c-axis. On the other hand, post-He plasma treatment changes the orientation of the ZnO crystal. It might decrease the electrical resistivity.

(5) In FE-SEM observation, conic shaped crystal grains of various sizes were observed on the cross sectional view of as-deposited ZnO film. Gaps exist between them. However, gaps disappeared and the grain columns were tightly packed with a smooth surface after post-He plasma treatment. This smooth shape might cause high mobility, which is good for reducing resistivity.

These results suggest that the post-He plasma treatment changes the microstructure of the film and causes electrical resistivity to decrease. However, the resistivity was still higher than our goal. In the future, more experiments into reducing resistivity are needed.

Acknowledgements

This work was supported by JKA and its promotion funds from KEIRIN RACE.

References

1) W. Li, Y. Li, G. Du, N. Chen, S. Liu, S. Wang, H. Huang, C. Lu and X. Niu, "Enhanced alectrical and optical properties of boron-doped ZnO films grown by low pressure chemical vapor deposition for amorphous silicon copar cells", *Ceramics Int.*, **42** (2016) 1361-1365.

2) A. Abrutis, L. Silimavicius, V. Kubilius, T. Murauskas, Z. Saltyte and V. Plausinaitiene, "Doped zinc oxide films grown by hot-wire chemical vapor deposition", *Thin Solid Films*, **576** (2015) 88-97.

3) Y. Natsume, H. Sakata and T. Hirayama, "Low-temperature electrical conductivity and optical absorption edge of ZnO films prepared by chemical vapor deposition", *Physica Status Solidi*, **A148** (1995) 485-495.

4) C. Chao, P. Chi and D. Wei, "investigations on the crystallographic orientation induced surface morphology evolution of ZnO thin films and their wettabillity and conductivity", *J. Phys. Chem.* C, **120** (2016) 8210-8219.

5) S. J. Lim, S. Kwon and H. Kim, "ZnO thin films prepared by atomic layer deposirion and rf sputtering as an active layer for thin film transistor", *Thin Solid Films*, **516** (2008) 1523-1528.

6) Y. Suzaki, S. Ejima, T. Shikama, S. Azuma, O. Tanaka, T. Kajitani and H. Koinuma, "Deposition of ZnO film using an open-air cold plasma generator", *Thin Solid Films*, **506-507** (2006) 155.

7) Y. Suzaki, A. Kawaguchi, T. Murase, T. Yuji, T. Shikama, D. B. Shin and Y. K. Kim, "Effect of substrate temperature on ZnO thin film fabrication by using an atmospheric pressure cold plasma generator", *Physica Status Solidi*, **C8** (2011) 503-505.

8) D. B. Shin, A. Kawaguchi, T. Murase, T. Yuji, T. Shinkama, Y. K. Kim and Y. Suzaki, "Optical Emission Spectroscopy of Atmospheric Pressure Cold Plasma and Fabrication of ZnO Films", *Frontier of Applied Plasma Technology*, **3** (2010) 126-129.

9) C. Lee and M. Choi, "Effects of the deposition on the microstructure and properties of ZnO thin films deposited by metal organic chemical vapor deposition with ultrasonic nebulization", *Thin Solid Films*, **605** (2016) 157-162.

10) Y. Nose, T. Yoshimura, A. Ashida, T. Uehara and N. Fujimura, "Novel chemical vapor deposition process of ZnO films using nonequilibrium N_2 plasma generated near atmospheric pressure with small amount of O_2 below 1%", *J. Appl. Phys.* **119** (2016) 175302/1-175302/6.

11) Y. Suzaki, X. Ma, T. Yuji and K.Yamauchi, "Effect of post-annearing in nitrogen gas on the microstructure of ZnO thin films prepared using atmospheric pressure cold plasma", *Frontier of Applied Plasma Technology*, **9** (2016) 61-65.

12) F. Lotgering, "Topotactical reactions with ferromagnetic oxides having hexagonal crystal structures-I", *J. Inorg. Nucl. Chem.* **9** (1959) 113-123.

13) "Powder Diffraction File", Sets 35-36, Inorgnic, International Center for Diffraction Data (1990) p.1048.